

PERFORMANCE ANALYSIS OF SPACE-TIME CODED MIMO-OFDM SYSTEMS UNDER I/Q IMBALANCE

Yaning Zou, Mikko Valkama, and Markku Renfors

Tampere University of Technology
Institute of Communications Engineering
P.O. Box 553, FIN-33101 Tampere, FINLAND

ABSTRACT

The combination of orthogonal frequency division multiplexing (OFDM) and multiple-input multiple-output (MIMO) techniques has been widely considered as the most promising approach for building future wireless transmission systems. In such systems, the limited implementation resources for the radio parts cause big restrictions on the size, cost, and quality of the individual radio transceivers. This implies that there are several imperfections at the analog radio front-end stages, which in turn can severely limit the overall system performance. One good example is the so called I/Q imbalance problem related to the amplitude and phase matching of the transceivers I and Q chains. This paper studies the performance of space-time coded (STC)-OFDM systems under I/Q imbalance. As a practical example, a 2×1 STC-OFDM system is examined in detail and a closed-form solution for the resulting signal-to-interference ratio (SIR) due to I/Q imbalance at the output of the receiver combining stage is derived. The analytical outcomes are verified using extensive computer simulations, and can easily be extended to multi-antenna receiver cases as well. In general, the obtained results indicate that I/Q imbalance can easily become a limiting factor in practical STC-OFDM systems and should be carefully mitigated using proper digital and/or analog signal processing.

Index Terms — Complex (I/Q) signals, digital radios, direct-conversion transceivers, I/Q imbalance, MIMO, OFDM, signal-to-interference ratio, space-time coding

1. INTRODUCTION

The limited spectral resources and the fast-rising demands on system throughput and network capacity are generally seen as the main driving force in the development and evolution of future wireless communication systems. It is crucial to find means of improving system performance in terms of the overall spectral efficiency as well as individual link quality [1]-[2]. One of the most promising methods is to generate parallel “data pipes” by utilizing multiple transmit and receive antennas, proper space-time coding, and the multi-path propagation phenomenon of the physical radio channels. The constructed transmission matrix enables a number of ways to efficiently improve throughput and system capacity as well as the link quality. On the other hand, to achieve higher absolute data rates, wider signaling bandwidths will also be used. But wide-band channels are much more difficult to be dealt with than their narrowband counterparts. One efficient solution for taking use of and coping with the wideband radio channels is then to use OFDM [1], [2]. By converting the overall frequency-selective channel into a collection of parallel frequency-flat subchannels, OFDM modulation takes advantage of the frequency diversity in multi-path envi-

ronments. Therefore, when targeting for spectral efficiencies in the order of 10 bits/s/Hz and absolute data rates at 100 Mbits/s range in the emerging wireless systems [1], [2], the combination of multi-antenna techniques and OFDM has generally drawn wide attention in communications and signal processing research communities.

While there has been lots of communication theoretic interest in multi-antenna transmission techniques, the actual radio implementation related issues have not been thoroughly investigated yet. With multiple transmit and/or receive antennas, also multiple radio implementations are needed, and the limited overall implementation resources cause big restrictions on the size and cost of individual radios. Based on this, the individual radio implementations have several non-idealities which can cause considerable decrease in the overall system performance if not taken properly into account. One important practical example is the so called I/Q imbalance problem [3], [4], stemming from the unavoidable differences in the amplitudes and phases of the physical analog I and Q signal paths. In this paper, we continue the work in [5] by analytically assessing the signal degradation due to I/Q imbalance in the STC-OFDM system context with the individual radios being based on the direct-conversion radio architecture. Under I/Q imbalance on both the transmitter and receiver sides, the performance of a 2×1 STC-OFDM system is examined analytically, in terms of the obtainable signal-to-interference ratio (SIR) due to I/Q errors. It should be noted that multi-antenna OFDM system performance under I/Q imbalances has also been evaluated in [6]-[10], but only using computer simulations. Here the emphasis is on analytical SIR analysis, similar to that in [5], where single-carrier STC systems were considered, or in [11] in which ordinary OFDM is assumed. In general, the obtained analysis results demonstrate that in practical frequency-selective radio channels, the achievable SIR values on active subcarriers are different and depend on the actual power-delay profile of the radio channels. Furthermore, the SIR analysis results can be used to predict the high SNR behavior of the detection error probabilities without resorting to lengthy system simulations. Thus in general, these analysis results establish a solid analytical foundation for fully understanding and appreciating the I/Q imbalance effects on the performance of STC-OFDM systems, both from the system level as well as receiver signal processing algorithm designer point of views.

2. SPACE-TIME CODED (STC)-OFDM SYSTEMS AND I/Q IMBALANCES

2.1 STC-OFDM Transmission

A multi-antenna system utilizing 2×1 Alamouti transmit diversity scheme [12] combined with OFDM is considered here. As shown in Fig. 1, the space-time coding is applied separately for each sub-carrier data stream and then transmitted using two parallel OFDM transmitters. On the receiver side, the diversity combining is then applied over two consecutive OFDM symbol intervals.

This work was supported by the Technology Industries of Finland Centennial Foundation, the Academy of Finland, and the Graduate School TISE.

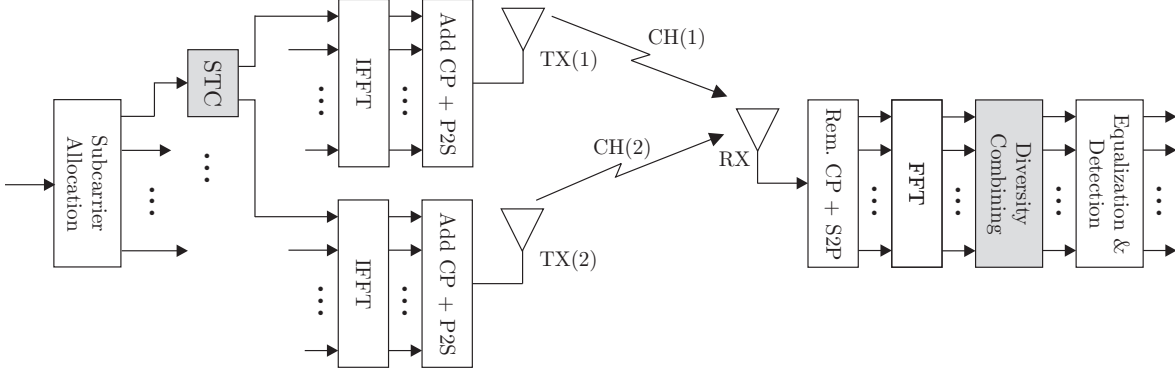


Fig. 1. Space-time coded (STC) 2x1 transmit diversity OFDM system.

Let $s_1(k)$ and $s_2(k)$ represent the two consecutive data samples to be transmitted over the k -th subcarrier. Assuming the guard interval (GI) implemented as a cyclic prefix (CP) is longer than the channel delay spread, the corresponding samples at the outputs of the receiver fast Fourier transform (FFT) stage after CP removal are given by

$$\begin{aligned} x_1(k) &= H_1(k)s_1(k) + H_2(k)s_2(k) \\ x_2(k) &= -H_1(k)s_2^*(k) + H_2(k)s_1^*(k) \end{aligned} \quad (1)$$

Here $H_1(k)$ and $H_2(k)$ denote the channel frequency responses (TX(1)→RX and TX(2)→RX) at subcarrier k , and additive noise is ignored for simplicity. Then assuming ideal channel knowledge, the receiver combines the two observations as

$$\begin{aligned} y_1(k) &= H_1^*(k)x_1(k) + H_2(k)x_2^*(k) = (|H_1(k)|^2 + |H_2(k)|^2)s_1(k) \\ y_2(k) &= H_2^*(k)x_1(k) - H_1(k)x_2^*(k) = (|H_1(k)|^2 + |H_2(k)|^2)s_2(k) \end{aligned} \quad (2)$$

which yields diversity gain over the individual links as is obvious. Given amplitude modulated data, like QAM, the observations need to be scaled by the inverse of $H(k) = |H_1(k)|^2 + |H_2(k)|^2$ before the actual data detection stage.

2.2 Transmitter and Receiver I/Q Imbalance Models

Let $z(t) = z_I(t) + jz_Q(t)$ denote the complex baseband equivalent signal to be transmitted. On the transmitter side, the imbalanced (upconversion) local oscillator (LO) signal model is $x_{LO}^T(t) = \cos(\omega_C t) + jg_{TX} \sin(\omega_C t + \phi_{TX})$ where ω_C denotes the RF carrier frequency, and g_{TX} and ϕ_{TX} model the transmitter amplitude and the phase imbalances, respectively. Then assuming the direct-conversion radio architecture is applied, the baseband equivalent signal with I/Q imbalance is of the form

$$z_{TX}(t) = K_{1, TX}z(t) + K_{2, TX}z^*(t) \quad (3)$$

Here the imbalance coefficients are given by $K_{1, TX} = (1 + g_{TX}e^{j\phi_{TX}})/2$ and $K_{2, TX} = (1 - g_{TX}e^{-j\phi_{TX}})/2$. Similarly, the imbalanced (downconversion) LO signal on the receiver side can be written as $x_{LO}^R(t) = \cos(\omega_C t) - jg_{RX} \sin(\omega_C t + \phi_{RX})$ where g_{RX} models the amplitude and ϕ_{RX} the phase imbalance, respectively. The corresponding imbalanced baseband equivalent observation $z_{RX}(t)$ is then of the form

$$z_{RX}(t) = K_{1, RX}z(t) + K_{2, RX}z^*(t) \quad (4)$$

where the corresponding imbalance coefficients are of the form $K_{1, RX} = (1 + g_{RX}e^{-j\phi_{RX}})/2$ and $K_{2, RX} = (1 - g_{RX}e^{j\phi_{RX}})/2$.

The previous models in (3) and (4) are general imbalance models and used extensively in the literature, see, e.g., [5], [8], [10] and the references therein. In the context of OFDM systems, it is also very important to understand the I/Q imbalance effects in frequency domain. Taking (3) and (4) into frequency domain yields

$$Z_{TX}(k) = K_{1, TX}Z(k) + K_{2, TX}Z^*(-k) \quad (5)$$

$$Z_{RX}(k) = K_{1, RX}Z(k) + K_{2, RX}Z^*(-k) \quad (6)$$

where k refers to the subcarrier frequency (index). This results in intercarrier interference (ICI) between the mirror-subcarrier pairs and is the most important characteristic of the I/Q imbalance effects in OFDM based systems.

2.3 Overall STC-OFDM System Model

Incorporating the transmitter and receiver I/Q imbalances into the system setup shown in Fig. 1, the observations at the output of the diversity combining stage at subcarrier k (except for $k = -N/2$ and 0 where N denotes the IFFT/FFT size) appear as

$$\begin{aligned} y_1(k) &= a(k)s_1(k) + b(k)s_1^*(-k) + c(k)s_2(k) + d(k)s_2^*(-k) \\ y_2(k) &= a^*(k)s_2(k) + b^*(k)s_2^*(-k) - c^*(k)s_1(k) - d^*(k)s_1^*(-k) \end{aligned} \quad (7)$$

Here the exact expressions for the coefficients $a(k)$, $b(k)$, $c(k)$ and $d(k)$ are given in (8) (next page). Thus the observations at subcarrier k are interfered by the conjugate of the data at the corresponding mirror carrier $-k$ as well as by the other data symbol within the STC block at subcarriers k and $-k$. Similar to the single-carrier system analysis in [5], the above system model in (7) can be extended to the corresponding $2 \times M$ diversity scheme where the coefficients $a(k)$, $b(k)$, $c(k)$ and $d(k)$ have more complicated expressions due to the additional receiver antennas.

Closer comparison of the above system model with its single-carrier counterpart in [5] reveals some further differences. Assuming independent subcarrier data streams, the combiner outputs here appear as weighted linear combinations of 4 independent data symbols, while in the corresponding single-carrier system there are only two independent data symbols and their own complex-conjugates. This has rather big impact on the distribution of the overall interference, and is thus important when carrying out the statistical interference analysis in the continuation. Another difference lies in the structure of the coefficients $a(k)$, $b(k)$, $c(k)$ and $d(k)$ which, for any subcarrier k , are influenced also by the channel frequency responses at subcarrier $-k$. Therefore, if the channel is frequency-selective, the I/Q imbalance effects become much more complicated than in the corresponding single-carrier case

$$\begin{aligned}
a(k) &= |H_1(k)|^2 K_{1,RX} K_{1,TX(1)} + H_1^*(k) H_1^*(-k) K_{2,RX} K_{2,TX(1)} + |H_2(k)|^2 K_{1,RX}^* K_{1,TX(2)} + H_2(k) H_2(-k) K_{2,RX}^* K_{2,TX(2)} \\
b(k) &= |H_1(k)|^2 K_{1,RX} K_{2,TX(1)} + H_1^*(k) H_1^*(-k) K_{2,RX} K_{1,TX(1)} + |H_2(k)|^2 K_{1,RX}^* K_{2,TX(2)} + H_2(k) H_2(-k) K_{2,RX}^* K_{1,TX(2)} \\
c(k) &= H_1^*(k) H_2(k) K_{1,RX} K_{1,TX(2)} + H_1^*(k) H_2^*(-k) K_{2,RX} K_{2,TX(2)} - H_1^*(k) H_2(k) K_{1,RX}^* K_{1,TX(1)} - H_1(-k) H_2(k) K_{2,RX}^* K_{2,TX(1)} \\
d(k) &= H_1^*(k) H_2(k) K_{1,RX} K_{2,TX(2)} + H_1^*(k) H_2^*(-k) K_{2,RX} K_{1,TX(2)} - H_1^*(k) H_2(k) K_{1,RX}^* K_{2,TX(1)} - H_1(-k) H_2(k) K_{2,RX}^* K_{1,TX(1)}
\end{aligned} \tag{8}$$

discussed in [5]. These will be verified and demonstrated by both analysis as well as numerical illustrations and computer simulations in the next sections.

3. SIGNAL-TO-INTERFERENCE RATIO (SIR) ANALYSIS

In the following, we analyze the performance degradation under I/Q imbalance in terms of signal-to-interference ratio (SIR) at the combiner output using the signal models of the previous section. We assume L -tap frequency-selective radio channels with the individual taps being modeled as independent circular complex Gaussian random variables with zero mean and power profile $\mathbf{P} = [P(0), P(1), \dots, P(L-1)]^T$ where $P(l)$ denotes the power of the l -th tap. Based on this, it is easy to show that the channel frequency responses $H_1(k)$ and $H_2(k)$ at subcarrier k are also complex circular Gaussian random variables with zero mean and equal mean power $E[|H_1(k)|^2] = E[|H_2(k)|^2] = \sum_{l=0}^{L-1} P(l) = P_H$. Then it also follows that

$$\begin{aligned}
a) \quad & E[H_1^2(k)] = E[H_2^2(k)] = 0 \\
b) \quad & E[H_1(k)H_1(-k)] = E[H_2(k)H_2(-k)] = 0 \\
c) \quad & E[H_1(k)H_1^*(-k)] = E[H_2(k)H_2^*(-k)] = \sum_{l=0}^{L-1} P(l) e^{-j4\pi k l / N} \\
d) \quad & E[|H_1(k)|^4] = E[|H_2(k)|^4] = 2P_H^2 \\
e) \quad & E[|H_1(k)|^2 H_1^2(k)] = E[|H_2(k)|^2 H_2^2(k)] = 0
\end{aligned}$$

which simplifies the following analysis.

Now consider the first combiner output $y_1(k)$ in (7) where the first term is the desired signal term while the other three terms act as interference. Then assuming that the symbols $s_1(k)$, $s_2(k)$, $s_1(-k)$ and $s_2(-k)$ are all equal-variance, uncorrelated, circular complex random variables, independent of the channel coefficients, the SIR at subcarrier k can be defined as

$$SIR(k) = \frac{E[|a(k)/H(k)|^2]}{E[|b(k)/H(k)|^2] + E[|c(k)/H(k)|^2] + E[|d(k)/H(k)|^2]} \tag{9}$$

where $H(k) = |H_1(k)|^2 + |H_2(k)|^2$. Based on (7) and the previous assumptions, (9) holds also for the second combiner output $y_2(k)$, and can also be extended easily to $2 \times M$ STC transmit diversity cases. Direct simplification of the above SIR expression is somewhat tedious due to the intercarrier interference between mirror-sub-carriers. The SIR also varies as a function of the subcarrier index k and depends on the power-delay profile of the radio channels.

To get some general understanding on the role of the channel type, we examine next two extreme cases further – (i) frequency-flat (single-tap) channel and (ii) arbitrarily frequency-selective (infinite delay spread) channel. In the first case, the channel frequency response values are identical for all the subcarriers while in the second case, the different subcarriers fade totally independently. This results in a range of SIR values SIR_{\max} and SIR_{\min} within which $SIR(k)$ in (9) is then located with practical channels. After some manipulations, these SIR bounds corresponding to the previous cases can be formulated as

$$SIR_{\min} \approx SIR_{def}(3,3), \quad SIR_{\max} \approx SIR_{def}(2,1) \tag{10}$$

where

$$SIR_{def}(\alpha_1, \alpha_2) = A(\alpha_1) / B(\alpha_1, \alpha_2) \tag{11}$$

and $A(\alpha_1)$ and $B(\alpha_1, \alpha_2)$ are given in (12) (next page). In general, the values of α_1 and α_2 depend on the channel power-delay profiles and the values shown in (10) correspond to the previous extreme cases (i) and (ii). As a concrete practical example, assume that the imbalance values of the two transmitters and one receiver are 4%, -4° (TX1), 3%, 3° (TX2), and 5%, 5° (RX). This represents a realistic example case from the radio front-end design point of view. Using (10)-(12), the feasible range of SIR values is then from 21dB to 22.7dB. Further illustrations with practical fading multipath channels will be given in Section 4.

3.1 Interpretation of SIR and Nature of Interference

The previous analysis led to a closed-form solution for the power ratio of the desired signal and interfering signal terms due to I/Q imbalance. This SIR depends only on the type of the communications channel and, of course, the transmitters and receiver I/Q imbalance values, and can be evaluated directly without any system- or link-level data simulations. The SIR value itself, in turn, forms an upper bound for the overall signal-to-interference-and-noise ratio (SINR) that can be achieved in the transmission chain at the detector input. Even though the exact probability distribution of the combined interference terms $b(k)s_1^*(-k) + c(k)s_2(k) + d(k)s_2^*(-k)$ and $b^*(k)s_2^*(-k) - c(k)s_1(k) - d^*(k)s_1^*(-k)$ in (7) is not Gaussian, the Gaussian *approximation* is still feasible with high-order data modulations since the interference terms appear as weighted linear combinations of three independent subcarrier symbols. Thus the SIR representing an upper bound for the SINR can then be mapped to lower bound on the achievable detection error rate. Even though this is a crude approximation from the interference distribution point of view, it will be shown by simulations to hold from the error rate point of view in the next Section.

4. SIMULATIONS AND ILLUSTRATIONS

In this section, the previous analysis results are illustrated using computer simulations. 64-QAM data modulation is used and the number of OFDM subcarriers is $N = 64$. Two different power-delay profiles with $\mathbf{P}_1^{dB} = \{0, -1.85, -3.64, -5.45\}$ and $\mathbf{P}_2^{dB} = \{0, -1.85, -\infty, -\infty, -\infty, -3.64, -\infty, -5.45\}$ are examined where the delay spacing is equal to IFFT/FFT sample duration ($N = 64$ -th part of the OFDM symbol duration). Proper cyclic prefix (CP) is always used on the transmitter side and discarded in the receiver prior to the FFT. The channel tap realizations are chosen independently from complex Gaussian distribution and assumed constants over two consecutive OFDM symbol periods [12] after which new channel realizations are drawn. The previous I/Q imbalance values of 4%, -4° (TX1), 3%, 3° (TX2), and 5%, 5° (RX) are used, yielding the theoretical SIR range of 21dB to 22.7dB as stated earlier. The corresponding individual image attenuations are roughly 28dB, 30.4dB and 26dB, respectively. The overall amount of data symbols transmitted through the system is 500,000.

$$\begin{aligned}
A(\alpha_1) &= 2 \sum_{i=1}^2 |K_{1,RX} K_{1,TX(i)}|^2 + \alpha_1 \sum_{i=1}^2 |K_{2,RX} K_{2,TX(i)}|^2 + 2 \operatorname{Re}[K_{1,RX}^2 K_{1,TX(1)} K_{1,TX(2)}] \\
B(\alpha_1, \alpha_2) &= 3 \sum_{i=1}^2 |K_{1,RX} K_{2,TX(i)}|^2 + (\alpha_1 + \alpha_2) \sum_{i=1}^2 |K_{2,RX} K_{1,TX(i)}|^2 + \sum_{i=1}^2 |K_{1,RX} K_{1,TX(i)}|^2 + \alpha_2 \sum_{i=1}^2 |K_{2,RX} K_{2,TX(i)}|^2 \\
&\quad - 2 \operatorname{Re}[K_{1,RX}^2 K_{1,TX(1)} K_{1,TX(2)}]
\end{aligned} \tag{12}$$

First, with the two practical channel power-delay profiles \mathbf{P}_1 and \mathbf{P}_2 , the average subcarrier-wise SIR is evaluated numerically with 50,000 independent channel realizations, by calculating sample averages for the signal and interference powers. The obtained SIR values are depicted in Fig. 2. Clearly, the analytical SIR results predict the SIR behavior very accurately. Then the actual bit error rate (BER) of the whole transmission system is evaluated, with and without the previous I/Q imbalances, assuming channel profile \mathbf{P}_2 . The results are depicted in Fig. 3 as a function of average signal-to-noise ratio (SNR) due to channel noise at the detector input. The figure also shows the BER values corresponding to the derived SIR values of 21dB and 22.7dB. Obviously, the analysis predicts accurately the BER floor due to I/Q imbalance.

5. CONCLUSIONS

This paper studied the impact of transmitter and receiver I/Q imbalances on the performance of space-time coded OFDM systems. Average signal-to-interference ratio due to I/Q errors was derived analytically, assuming Gaussian fading channels. Two extreme cases were considered in detail, with either frequency-flat or independent subcarrier fading characteristics, within which the practical fading and multipath profiles then fit. The derived SIR value gives an upper bound on the achievable signal-to-interference-and-noise ratio (SINR) in the overall system prior to data detection, and can be used to assess the role of I/Q imbalances on the system performance without lengthy data and system simulations. The analysis also verifies that I/Q imbalance is relatively even a bigger problem in multi-antenna OFDM systems than in their traditional single-antenna single-carrier counterparts.

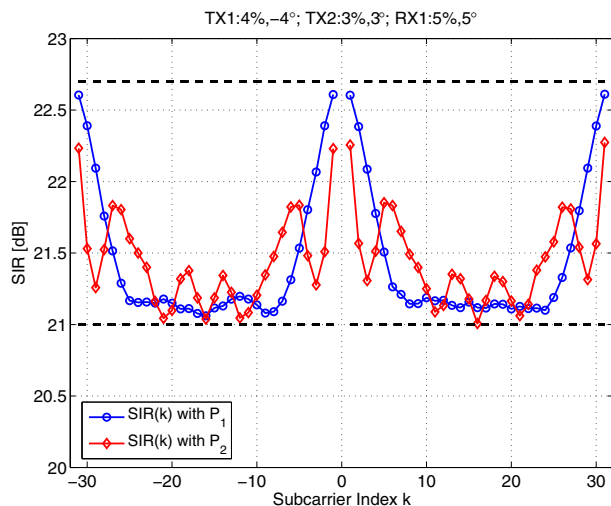


Fig. 2. SIR as a function of the subcarrier index k with two different channel power-delay profiles \mathbf{P}_1 and \mathbf{P}_2 . The dashed lines show the analytical SIR values corresponding to the frequency-flat (upper dashed line) and independently fading subcarrier cases (lower dashed line), respectively.

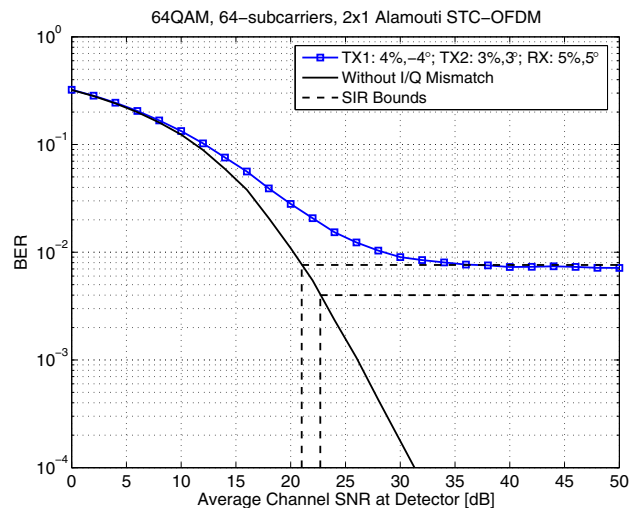


Fig. 3. 64-QAM bit error rate with and without I/Q imbalance.

6. REFERENCES

- [1] R. Tafazolli, Ed., *Technologies for the Wireless Future: Wireless World Research Forum (WWRF)*. Chichester, U.K.: Wiley, 2004.
- [2] H.-H. Chen, M. Guizani, and J. F. Huber, Eds., "Multiple access technologies for B3G wireless communications," *IEEE Commun. Mag.*, vol. 43, Feb. 2005.
- [3] B. Razavi, *RF Microelectronics*. Englewood Cliffs, NJ: Prentice-Hall, 1998.
- [4] S. Mirabbasi and K. Martin, "Classical and modern receiver architectures," *IEEE Commun. Mag.*, vol. 38, pp. 132-139, Nov. 2000.
- [5] M. Valkama, Y. Zou, and M. Renfors, "On I/Q imbalance effects in MIMO space-time coded transmission systems," in *Proc. IEEE Radio Wireless Symp.*, San Diego, CA, Jan. 2006, pp. 223-226.
- [6] J. Liu *et al.*, "Impact of front-end effects on the performance of downlink OFDM-MIMO transmission," in *Proc. IEEE Radio Wireless Conf.*, Atlanta, GA, Sept. 2004, pp. 159-162.
- [7] R. M. Rao and B. Daneshrad, "I/Q mismatch cancellation for MIMO-OFDM systems," in *Proc. IEEE Int. Symp. Pers., Indoor, Mobile Radio Commun.*, Barcelona, Spain, Sept. 2004, pp. 2710-2714.
- [8] T. C. W. Schenk, P. F. M. Smulders, and E. R. Fledderus, "Estimation and compensation of TX and RX IQ imbalance in OFDM-based MIMO systems," in *Proc. IEEE Radio Wireless Conf.*, San Diego, CA, Jan. 2006, pp. 215-218.
- [9] H. Kamata, K. Sakaguchi, and K. Araki, "An effective IQ imbalance compensation scheme for MIMO-OFDM communication system," in *Proc. IEEE Int. Symp. Pers., Indoor, Mobile Radio Commun.*, Berlin, Germany, Sept. 2005.
- [10] A. Tarighat and A. H. Sayed, "MIMO OFDM receivers for systems with IQ imbalances," *IEEE Trans. Signal Processing*, vol. 53, pp. 3583-3596, Sept. 2005.
- [11] A. Tarighat, R. Bagheri, and A. H. Sayed, "Compensation schemes and performance analysis of IQ imbalances in OFDM receivers," *IEEE Trans. Signal Processing*, vol. 53, pp. 3257-3268, Aug. 2005.
- [12] S. M. Alamouti, "A simple transmit diversity technique for wireless communications," *IEEE J. Selected Areas Commun.*, vol. 16, pp. 1451-1458, Oct. 1998.